Article

Transverse Pressure Induced Phase Transitions in Boron Nitride Nanotube Bundles and the Lightest Boron Nitride Crystal

Shaogang Hao, Gang Zhou, Wenhui Duan, Jian Wu, and Bing-Lin Gu

J. Am. Chem. Soc., **2008**, 130 (15), 5257-5261 • DOI: 10.1021/ja7107678 • Publication Date (Web): 26 March 2008

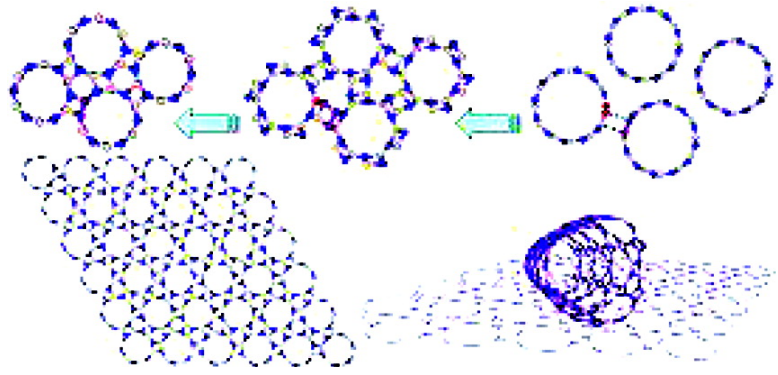

J|A|C|S
ARTICLES

Published on Web 03/26/2008

Transverse Pressure Induced Phase Transitions in Boron Nitride Nanotube Bundles and the Lightest Boron Nitride Crystal

Shaogang Hao,[†] Gang Zhou,[†] Wenhui Duan,*[,†] Jian Wu,[‡] and Bing-Lin Gu[‡]

Department of Physics, Tsinghua University, and Center for Advanced Study, Tsinghua University, Beijing 100084, People's Republic of China

Received December 3, 2007; E-mail: dwh@phys.tsinghua.edu.cn

Abstract: We simulate the phase transition processes of aligned crystalline boron nitride (BN) nanotube bundles under transverse pressure, and investigate the phase transition mechanism and transition conditions. The *antiparallel polar bonds rule*, associated with the interaction between the tubes, is demonstrated to be crucial to such phase transitions. And the curvature of the tubes can greatly affect the phase transition behavior. We discover a unique $sp^2-sp^3-sp^2$ transition and a series of new BN crystal phases including a novel porous sheet-stacking-up form with the lightest density (2.01 g/cm^3), which could be used in highly efficient energy storage.

1. Introduction

Boron nitride (BN) has two representative crystal structures. One is the sheet-stacking-up hexagonal form (*h*-BN) with in-plane trigonal sp^2 bonding. The other is the highly dense cubic form (*c*-BN) with tetrahedral sp^3 bonding. One decade ago, a one-dimensional (1D) form, BN nanotube (BNNT), was fabricated out,[1] following the pioneering theoretical prediction.[2] BNNT has the hollow tubular structure as rolling up of the *h*-BN sheets. Due to the intertube van der Waals attraction, nanotubes are usually produced in bundle forms.[3–6] Nowadays, nanotube bundles are not only the basis of many fundamental and significant designs in electronic devices and functional materials (such as super tough fiber, field effect transistor, field emission display, etc),[6–10] but also are ideal media for atomic (e.g., Li, H, and inert gases) or molecular (e.g., H_2) storage.[6,11] And a great deal of theoretical and experimental efforts have focused on the structures and properties of carbon nanotube bundles (CNTBs) at the ground state[12] or under pressure.[13] It is revealed that the CNTBs only undergoes a series of *shape* transitions under hydrostatic pressure, and strictly, no well-defined new phase appears,[13] while the story may be quite different for BNNT bundles (BNNTBs), a representative of compound tubes. The B−N bonds in the BNNT are polar,[2,14,15] leading to more complicated and unique intertube interactions in BNNTBs[15] as compared to those in the CNTBs.[12,13] Such specific intertube interaction suggests the possibility of more diverse phase transitions in BNNTBs under external pressure, which could lead to new crystalline phases with unique structures, novel properties, and potential applications. Moreover, the thorough studies of the phase transition behavior and mechanism of BNNTBs under pressure is beneficial to gaining a deeper insight into the "bottom-up" method in producing 1D nanostructure-based materials.

[†] Department of Physics
[‡] Center for Advanced Study.

(1) Chopra, N. G.; Luyken, R. J.; Cherrey, K.; Crespi, V. H.; Cohen, M. L.; Louie, S. G.; Zettl, A. *Science* **1995**, *269*, 966.
(2) (a) Blase, X.; Rubio, A.; Louie, S. G.; Cohen, M. L. *Europhys. Lett.* **1994**, *28*, 335. (b) Rubio, A.; Corkill, J. L.; Cohen, M. L. *Phys. Rev. B* **1994**, *49*, 5081.
(3) (a) Iijima, S. *Nature* **1991**, *354*, 56. (b) Iijima, S.; Ichihashi, T. *Nature* **1993**, *363*, 603. (c) Banerjee, S.; Wong, S. S. *J. Am. Chem. Soc.* **2002**, *124*, 8940. (d) Saran, N.; Parikh, K.; Suh, D. S.; Munoz, E.; Kolla, H.; Manohar, S. K. *J. Am. Chem. Soc.* **2004**, *126*, 4462.
(4) (a) Lee, R. S.; Gavillet, J.; Lamy de la Chapelle, M.; Loiseau, A.; Cochon, J.-L.; Pigache, D.; Thibault, J.; Willaime, F. *Phys. Rev. B* **2001**, *64*, R121405. (b) Golberg, D.; Bando, Y. *Appl. Phys. Lett.* **2001**, *79*, 415.
(5) Remskar, M.; Mrzel, A.; Skraba, Z.; Jesih, A.; Ceh, M.; Demar, J.; Stadelmann, P.; Lvy, F.; Mihailovic, D. *Science* **2001**, *292*, 479.
(6) (a) Shimoda, H.; Gao, B.; Tang, X. P.; Kleinhammes, A.; Fleming, L.; Wu, Y.; Zhou, O. *Phys. Rev. Lett.* **2001**, *88*, 015502. (b) Dalton, A. B.; Collins, S.; Muoz, E.; Razal, J. M.; Ebron, V. H.; Ferraris, J. P.; Coleman, J. N.; Kim, B. G.; Baughman, R. H. *Nature* **2003**, *423*, 703.
(7) Xiao, K.; Liu, Y. Q.; Hu, P. A.; Yu, G.; Sun, Y. M.; Zhu, D. B. *J. Am. Chem. Soc.* **2005**, *127*, 8614.
(8) (a) Avouris, P. *Chem. Phys.* **2002**, *281*, 429. (b) Ghosh, S.; Sood, A. K.; Kumar, N. *Science* **2003**, *299*, 1042.
(9) (a) de Heer, W. A.; Châtelain, A.; Ugarte, D. *Science* **1995**, *270*, 1179. (b) Choi, W. B.; Chung, D. S.; Kang, J. H.; Kim, H. Y.; Jin, Y. W.; Han, I. T.; Lee, Y. H.; Jung, J. E.; Lee, N. S.; Park, G. S.; Kim, J. M. *Appl. Phys. Lett.* **1999**, *75*, 3129. (c) Kim, C.; Choi, Y. S.; Lee, S. M.; Park, J. T.; Kim, B.; Lee, Y. H. *J. Am. Chem. Soc.* **2002**, *124*, 9906.
(10) Baughman, R. H.; Zakhidov, A. A.; de Heer, W. A. *Science* **2002**, *297*, 787.
(11) (a) Talapatra, S.; Migone, A. D. *Phys. Rev. Lett.* **2001**, *87*, 206106. (b) Nikitin, A.; Ogasawara, H.; Mann, D.; Denecke, R.; Zhang, Z.; Dai, H.; Cho, K.; Nilsson, A. *Phys. Rev. Lett.* **2005**, *95*, 225507.
(12) (a) Tersoff, J.; Ruoff, R. S. *Phys. Rev. Lett.* **1994**, *73*, 676. (b) López, M. J.; Rubio, A.; Alonso, J. A.; Qin, L.-C.; Iijima, S. *Phys. Rev. Lett.* **2001**, *86*, 3056.
(13) (a) Peters, M. J.; McNeil, L. E.; Lu, J. P.; Kahn, D. *Phys. Rev. B* **2000**, *61*, 5939. (b) Tang, J.; Qin, L.-C.; Sasaki, T.; Yudasaka, M.; Matsushita, A.; Iijima, S. *Phys. Rev. Lett.* **2000**, *85*, 1887. (c) Chan, S.-P.; Yim, W. -L.; Gong, X. G.; Liu, Z. -F. *Phys. Rev. B* **2003**, *68*, 075404. (d) Sluiter, M. H. F.; Kawazoe, Y. *Phys. Rev. B* **2004**, *69*, 224111.
(14) Li, J.; Zhou, G.; Liu, H.; Duan, W. H. *Chem. Phys. Lett.* **2006**, *426*, 148.
(15) Zheng, F. W.; Zhou, G.; Hao, S. G.; Duan, W. H. J. *Chem. Phys.* **2005**, *123*, 124716.

In this work, through *ab initio* calculations, we study the phase transition processes of aligned crystalline BNNTBs under transverse pressure. We first probe the phase transition mechanism and the transition conditions for armchair and zigzag BNNTBs, which may be generalized to chiral BNNTBs and other kinds of compound nanotube bundles. Then we explore the effect of the nanotube curvature (or diameter) on the phase transition behavior. Finally, we present the structural, mechanical, and electronic properties of the *lightest* BN phase resulting from transversally pressing (6,6) BNNTB. This novel sheet-stacking-up porous BN material with smaller density and higher in-plane modulus superior to *h*-BN could have possible application in highly efficient energy storage.

2. Models and Methods

We built up aligned crystalline nanotube bundles by periodically repeating BNNTs [armchair (n,n), n = 3–9, and zigzag (6,0), (8,0), (9,0) ones] in two dimensions. Our *ab initio* calculations are performed within density-functional theory in the local density approximation.[16] We employ the ultrasoft pseudopotential method[17] with plane-wave basis as implemented in VASP.[18] The cutoff energy of plane-wave basis is 450 eV. Integration over the Brillouin zone is done using the Monkhorst−Pack scheme.[19] To get the ground arrangement of free bundles in advance, the nanotube's rotational degree of freedom about the tube axis is fully considered in the structural relaxation, following which the simulations of the squeezing process are performed by reducing the in-plane lattice constant a. The convergence criterion for the force on each atom is 0.01 eV/Å.

3. Results and Discussion

We first focus on the close-packed armchair (6,6) BNNTB. Herein the hexagonal lattice with one BNNT per unit cell is employed, like the carbon[12,13] and MoS_2[5] nanotube bundles. Such unit cell shares the same symmetry with the (6,6) tube. The cohesive energy versus lattice constant of the (6,6) bundle in Figure 1a illustrates that the isolated BNNTs would be bundled together spontaneously until a = 11.5 Å (a total energy minimum), corresponding to the intertube separation of ~3.36 Å, which is consistent with the experimental fact that the BNNTs are usually produced in bundle forms.[4] When the lattice constant a is decreased from ~11.5 Å, the total energy of system increases, and correspondingly, smooth tube walls begin buckling, and the intertube bonds begin to be formed. At a = 8.5 Å, the coordination number of each atom clearly changes from 3 to 4, showing that an energy-consuming sp^2-sp^3 transition (denoted as the first step of phase transition) is achieved (Figure 1b middle). Continuously decreasing a, each "tube" is elongated more and more greatly along the tube axis until those intratube B−N bonds which are not perpendicular to the tube axis (named as NPBs) get broken, and the in-plane B−N 12-member rings bond together, resulting in the formation of a new layered porous phase of BN (denoted as *hp*66-BN) at a = 6.75 Å (a and c of Figure 2). Importantly, this second step of phase transition (i.e., sp^3-sp^2 transition) has an exothermic process from a = 7.7 to 6.75 Å, which is absent in CNTBs. The calculated energy barrier of the whole $sp^2-sp^3-sp^2$ transition is 1.18 eV/atom, and the highest pressure needed for this transition is 242 kB at $a \approx 9$ Å. Different from the well-known phase transition in carbon and BN materials under high pressure (i.e., the typical sp^2-sp^3 transition from the layered phase to the highly condensed

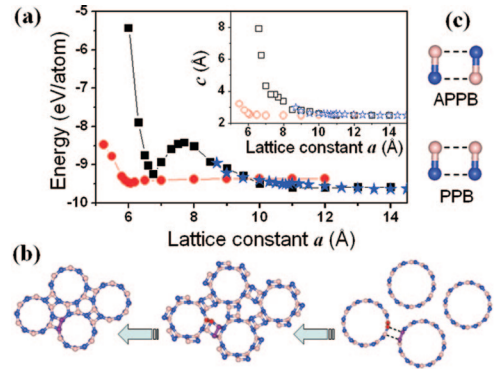

Figure 1. (a) Variations of cohesive energy and lattice constant c (inset) versus in-plane lattice constant a for (3,3) (circles), (6,6) (squares), and (8,8) (stars) BNNTBs. (b) Top view of atomic structures of (6,6) BNNTB at a = 11.0 (right), 8.5 (middle), and 6.75 Å (left). Red and purple bonds represent intratube B−N bonds that are not perpendicular to the tube axis and are perpendicular to the tube axis, respectively. Dashed lines illustrate an APPBs pair. (c) Patterns of APPBs and PPBs arrangement of two B−N polar bonds between adjacent tubes. Pink and blue balls represent B and N atoms, respectively.

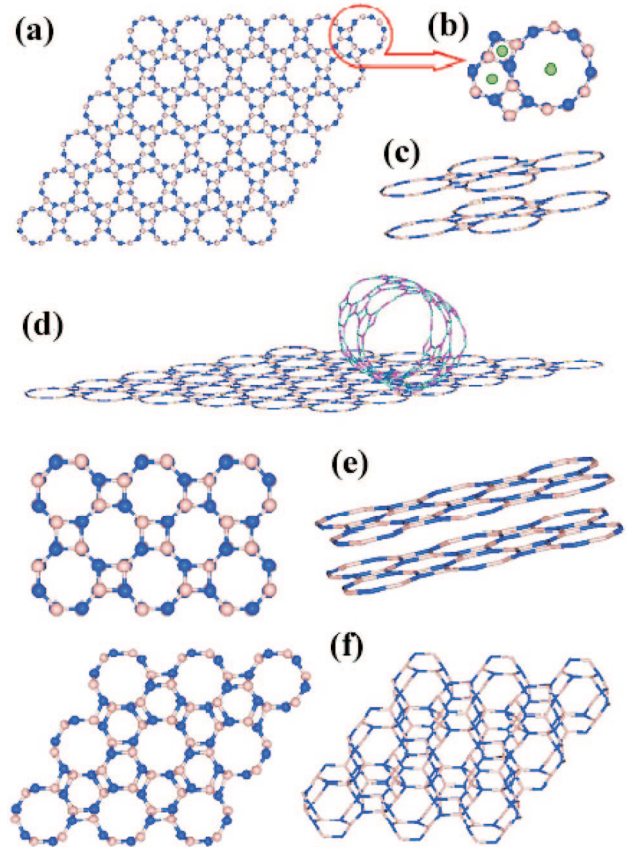

Figure 2. (a) Top view and (c) stereoview of the lightest BN crystal phase, *hp*66-BN. (b) Top view of three Li-doping sites: *h*4 at the interlayer tetragonal center, *h*6 at the interlayer hexagonal center, *h*12 at the in-plane dodecagonal center. Green ball represents Li atom. (d) The porous *hp*66-BNNT shown by rolling up the layered porous *hp*66-BN sheet. Top view and stereoview of (e) *tp*44-BN and (f) *hp*33-BN.

(16) Ceperley, D. M.; Alder, B. J. *Phys. Rev. Lett.* **1980**, *45*, 566.
(17) Vanderbilt, D. *Phys. Rev. B* **1990**, *41*, R7892.
(18) Kresse, G.; Furthmller, J. *Comput. Mater. Sci.* **1996**, *6*, 15.
(19) Monkhorst, H. J.; Pack, J. D. *Phys. Rev. B* **1976**, *13*, 5188 We use different converged sets of *k*-points for different lattice constants in the squeezing process.

phase),[20] here we find a unique $sp^2-sp^3-sp^2$ transition in the BNNTBs under transverse pressure, as shown in Figure 1b. The *hp*66-BN has the lightest density (2.01 g/cm^3) among all known BN crystals. The calculated cohesive energy of the *hp*66-BN is –9.24 eV/atom, higher than those of the isolated (6,6) BNNT (−9.59 eV/atom), the *h*-BN (−9.70 eV/atom), and the *c*-BN (−9.74 eV/atom), indicating that it is a metastable BN phase. Our *ab initio* molecular dynamics (MD) simulation, however, shows that the *hp*66-BN is stable even at 900 K[21] (see the Supporting Information). Moreover, we also repeat the squeezing process of armchair(6,6) BNNTB from $a = 11$ to 6.5 Å by using a two-times supercell along the tube axis. The phase transition behavior is almost the same as in the primary unit cell simulations, which shows the choice of the supercell (i.e., the lattice constant *c*) in our calculations does not affect the phase transition process and the production.

In the above phase transition process, the most remarkable character is the formation of the intertube polar (or heteronuclear) bonds under transverse pressure, which is never observed in the CNTBs.[13] This indicates that the nature of the intertube interaction and its variation in the pressing process play the crucial role in the phase transition of nanotube bundles. Generally, the former is dependent on the type (elemental and compound), component, composition (or chemical ratio), structure, and chirality of bundled nanotubes, while the latter is sensitive to the arrangement of bundles (see below). Actually, with the structural property of BNNTs, i.e., the B−N bond can be considered as the primary constituent of the BNNT, we can conveniently use the relative spatial orientations of polar B−N bonds of adjacent tubes to characterize the corresponding intertube interaction for the understanding of the intertube bonding character in bundles under transverse pressure: (1) For the antiparallel polar bonds (APPBs) arrangement between adjacent tubes (b and c of Figure 1), the external pressure can help the neighbor tubes to overcome the deformation energy to form the intertube bonds in the first step of phase transition, which is crucial for the subsequent new phase formation. (2) The parallel polar bonds (PPBs) arrangement (Figure 1c) results in the "frustrated" B−B and N−N bonds, rather than the intertube heteronuclear B−N bonds. Interestingly, the intertube bonding character in bundles under transverse pressure is quite similar to the bonding rules of BN fullerenes[22] and the growing BNNT edge.[23] It is easily understood that all of them have the common property determined by the constituents of BN materials, where the heteronuclear B−N bonds are energetically more favorable than the homonuclear B−B and N−N bonds. In what follows, we will elucidate in detail the APPBs rule of the nanotube arrangement, which enables the formation of intertube polar bonds in the phase transitions of armchair and zigzag nanotube bundles under transverse pressure.

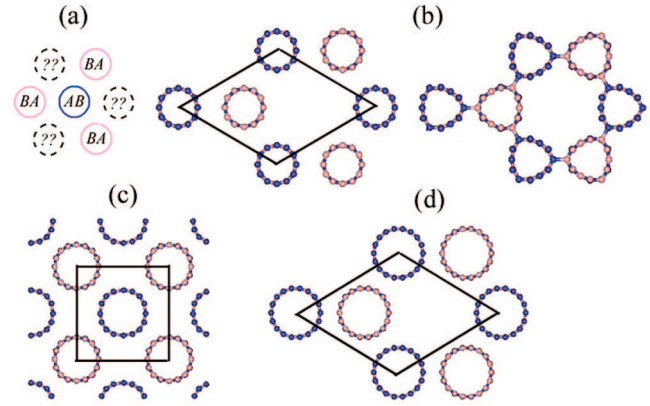

Figure 3. (a) Schematic top view of a hexagonal close-packed zigzag BNNTB. AB and BA indicate AB stacking and BA stacking, respectively. Dotted circle could be either AB or BA stacking. (b) Top views of initial (left) and self-aggregated (right) atomic structures of nonclose-packed (6,0) BNNTB. (c) and (d) Top view of nonclose-packed (8,0) and (9,0) BNNTBs after relaxation. The black frame in (b−d) indicates a unit cell which consists of two tubes.

For the armchair nanotube bundles, one of the most primary requirements of the APPBs rule is the symmetry matching between the tube and its bundle's lattice. As the transverse pressure is applied to the close-packed (4,4) BNNTB in the hexagonal lattice as to the (6,6) BNNTB, no stable, well-defined new phase is observed except for a series of structural deformations. The reason is that the APPBs rule cannot be well-satisfied in the hexagonal close-packed (4,4) BNNTB due to the mismatch between the symmetries of the tube (tetragonal symmetry) and the lattice (hexagonal symmetry), and thus, the intertube polar bonds can hardly be formed due to the unmatched intertube B−N orientation. However, when the simulation cell is changed from the hexagonal to the tetragonal so that the APPBs rule is perfectly satisfied with symmetry matching, almost the same phase transition (i.e., $sp^2-sp^3-sp^2$ transition) occurs as in the (6,6) BNNTB. And another porous sheet-stacking-up BN phase with tetragonal lattice (denoted as *tp*44-BN) is formed, as shown in Figure 2e. It should be noted that for free (4,4) BNNTB, the hexagonal close-packed lattice is energetically preferred, with 67.9 meV/atom lower than the tetragonal lattice in cohesive energy. While imposing transverse pressure on the bundle, the tetragonal lattice is energetically more favorable than the hexagonal lattice. This suggests that under pressure, the initial hexagonal (4,4) BNNTB phase will transform into tetragonal phase first, then undergo the $sp^2-sp^3-sp^2$ transition. The corresponding transition energy barrier of the tetragonal (4,4) BNNTB is 1.18 eV/atom, the same as that of the hexagonal (6,6) BNNTB. For those tubes whose symmetries never match any two-dimensional crystal lattice symmetry, their bundles will never reach a well-defined new BN crystal phase under transverse pressure because the APPBs rule can not be satisfied, as is confirmed by our simulations on (5,5) and (7,7) BNNTBs.

In zigzag BNNTBs, the situation becomes more complicated. Except for the symmetry matching restriction, even number of tubes in each unit cell is another primary requirement ensuring the APPBs rule in bundles (as shown in Figure 3a). Actually, in the close-packed zigzag BNNTB, the atom of one tube and its nearest atoms of some neighbor tubes are of the same type (i.e., B ↔ B, N ↔ N) because of the same stacking order along the tube axis, which indicates a PPBs arrangement. For such close-packed zigzag (6,0) BNNTB, we simulate the same

(20) (a) Fahy, S.; Louie, S. G.; Cohen, M. L. *Phys. Rev. B* **1986**, *34*, 1191. (b) Fahy, S.; Louie, S. G.; Cohen, M. L. *Phys. Rev. B* **1987**, *35*, 7623. (c) Wentzcovitch, R. M.; Fahy, S.; Cohen, M. L.; Louie, S. G. *Phys. Rev. B* **1988**, *38*, 6191.
(21) In the MD simulation, we used Nos algorithm, a time step of 0.5 fs, and the total steps of 5000.
(22) (a) Xia, X.; Jelski, D. A.; Bowser, J. R.; George, T. F. *J. Am. Chem. Soc.* **1992**, *114*, 6493. (b) Seifert, G.; Fowler, P. W.; Mitchell, D.; Porezag, D.; Frauenheim, Th. *Chem. Phys. Lett.* **1997**, *268*, 352. (c) Flowler, P. W.; Rogers, K. M.; Seifert, G.; Terrones, M.; Terrones, H. *Chem. Phys. Lett.* **1999**, *299*, 359. (d) Alexandre, S. S.; Mazzoni, M. S. C.; Chacham, H. *Appl. Phys. Lett.* **1999**, *75*, 61.
(23) (a) Blase, X.; De Vita, A.; Charlier, J. -C.; Car, R. *Phys. Rev. Lett.* **1998**, *80*, 1666. (b) Hao, S. G.; Zhou, G.; Duan, W. H.; Wu, J.; Gu, B. -L. *J. Am. Chem. Soc.* **2006**, *128*, 8453.

pressing process as for armchair (6,6) BNNTB in the hexagonal lattice, and only observe some structural deformations as expected. Once the unit cell consists of two tubes with one AB stacking and the other one BA stacking as shown in Figure 3b, a new phase would be formed spontaneously due to the bundle geometry abiding by the APPBs rule. Its cross section shows a triangle network. All the corner atoms become sp^3-hybridized, leading to effective bonding between the tubes, while other atoms are still sp^2-hybridized.

Furthermore, within the APPBs rule, we find that the phase transition behavior of BNNTBs can be considerably influenced by the curvature of the tube. In general, the structural property of bundled tubes is dependent on the tube's diameter or curvature.[12] When rolling up *h*-BN sheets into small BNNTs such as armchair (3,3) BNNT,[25] the original planar σ bonds are greatly bent and strongly mixed with π components (i.e., the original sp^2 bonding is strongly mixed with sp^3 component). As a result, the formation of the intertube bonds is energetically preferred even without external pressure, as shown in Figure 1a. A highly dense new hexagonal phase, denoted as *hp*33-BN (Figure 2f), is formed by self-aggregation. While for larger armchair tubes, they are transversely softer than the thinner ones, so the polygonized cross sections would appear in their bundles.[12] We simulate the hexagonal (9,9) and tetragonal (8,8) BNNTBs with the same lattices as (6,6), and (4,4) BNNTBs, respectively. When squeezing the bundles, the intertube polar bonds are formed, but the cross section polygonization simultaneously releases the stress in these larger tubes. Without enough intratube stress, the intratube NPBs can hardly break, and the second step of phase transition (i.e., $sp^2-sp^3-sp^2$ transition) can never be achieved (as demonstrated by the cohesive energy curve in Figure 1a). Once the transverse pressure is released, they will transform back to the initially stable bundle states without intertube bonding. The larger the armchair tube is, the harder it is to have phase transition in its bundle form. This also holds true for zigzag BNNTBs. For example, we perform the same simulations on the tetragonal zigzag (8,0) and hexagonal (9,0) BNNTBs with two BNNTs per unit cell, as shown in c and d of Figure 3. The self-aggregation does not happen, and the obtained intertube separations of 2.76 and 2.81 Å indicate no chemical bonding between the tubes in (8,0) and (9,0) BNNTBs.

In the following, we will focus our study on the structure and properties of the *hp*66-BN, and also discuss its possible applications. The *hp*66-BN has a sheet-stacking-up form, where the layers are only weakly bonded together with an AB stacking as shown in Figure 2c. The out-of-plane lattice constant is 6.23 Å, comparable to those of the *h*-BN and graphite. Each sheet is constructed by the sp^2 bonds between the B and N atoms, and appears to be a porous network built up by the alternating tetragons and hexagons. The formed periodic 12-membered rings have alternating side lengths of 1.39 Å (shared with the tetragons) and 1.44 Å (shared with the hexagons), while the interring bond length is uniformly 1.48 Å. The porous BN sheet has six different kinds of bond angles: the N−B−N angles are 96.2° in the tetragons, 120.8° in the hexagons, and 143.0° in the 12-membered rings, respectively; in the same order, the B−N−B angles are 83.8°, 119.2°, and 157.0°, respectively. Our calculations show that the *hp*66-BN crystal has the smallest density (2.01 g/cm^3) as compared with other BN phases such as *h*-BN (2.40 g/cm^3) and *c*-BN (3.62 g/cm^3). The calculated in-plane modulus is 1.17 TPa, in the same order of those of the graphite sheet (1.06 TPa) and the *h*-BN (0.84 TPa). The *hp*66-BN is a *direct-band gap* semiconductor with the band gap of 3.99 eV, slightly smaller than those of *h*-BN (4.04 eV) and isolated (6,6) BNNTs (4.20 eV) calculated by us.[26]

Due to its layered porous atomic structure, the *hp*66-BN could have promising application in energy storage, like graphite.[27] Especially, its loose structure and small density (17% smaller than that of graphite) are of benefit to higher energy storage efficiency. As an example, we choose three possible sites *h*4, *h*6, *h*12 (Figure 2b) to study the doping possibility of lithium (Li) in the BN materials. While doping one Li atom per *hp*66-BN unit cell, these three sites are all found to be energetically favorable for Li-doping, with the doping energies being respectively, 0.30, 0.57, and 0.01 eV per Li atom. In addition, the unique, layered porous structure could be very advantageous for the reversible intercalation and deintercalation processes of foreign ions. On the other hand, based on the widely accepted concept that the covalent-bonded materials with layered structures (e.g., graphite and *h*-BN sheet) are promising to form the tubular counterparts (e.g., CNT and BNNT), a new type of porous BNNTs can be achieved by rolling up the porous BN sheets (Figure 2d). The calculated energy band gap of the novel porous *hp*66-BNNT is around 4.0 eV.

In our theoretical simulations, we construct the bundle models with uniform nanotubes. One may argue that in practical cases, the bundles are always composed of tubes of different chiralities, while the intrinsic physical origin of the pressure-induced phase transitions in BNNTBs is the intertube interaction instead of chirality. The microscopic APPBs rule is substantially chirality independent, which could be generalized for any chiral BNNTB in addition to armchair and zigzag ones. Therefore, although the APPBs rule is strict for the whole BNNTBs, it is very possible that the phase transition will occur under pressure in some local area of bundles, where the atomic configuration follows this rule. While, for the multiwalled BNNTBs under transverse pressure, the interwall interaction/bonding within the multiwalled tube should also be taken into account in addition to the intertube interaction/bonding between the outmost walls of the bundled tubes, which implies much more complex transition behavior. Nevertheless, in such a case, the bonding characters would still follow the APPBs or heteronuclear B−N bonding rule in essence, compatible with the common property of BN materials (i.e., the heteronuclear B−N bonds are energetically more favorable than the homonuclear B−B and N−N bonds), and thus the transition mechanism is expected to be similar to that of the single-walled BNNTBs.

4. Summary

In summary, our simulation shows a vivid example revealing the potential application of the "bottom-up" method in constructing new material phases by 1D nanostructures. We find

(24) Verstraete, M.; Charlier, J.-C. *Phys. Rev. B.* **2003**, *68*, 045423.
(25) (a) Xiang, H. J.; Yang, J. L.; Hou, J. G.; Zhu, Q. S. *Phys. Rev. B* **2003**, *68*, 035427.
(26) Zunger, A.; Katzir, A.; Halperin, A. *Phys. Rev. B* **1974**, *13*, 5560 All the calculated energy gaps in this work could be corrected by adding an upshift of 1.73 eV, while the conclusion that all the new BN phases are wide gap semiconductors remains valid.
(27) Winter, M.; Besenhard, J. O.; Spahr, M. E.; Novák, P. *Adv. Mater.* **1998**, *10*, 725.
(28) Corso, M.; Auwärter, W.; Muntwiler, M.; Tamai, A.; Greber, T.; Osterwalder, J. *Science* **2004**, *303*, 217.

that the BNNTBs can undergo unique phase transitions under transverse pressure. The APPBs rule is a crucial condition for such phase transition of crystalline BNNTBs. In addition to the APPBs rule, the tube's curvature can also greatly affect the phase transition behavior. Concomitant with the phase transitions in BNNTBs, we obtain a series of new BN crystal phases, specially including the lightest one with the density of only 2.01 g/cm^3, which could be used in highly efficient energy storage. Recently, Corso et al. reported the successful fabrication of BN nanomesh,[28] but the exact atomic structure is still unknown. Our work appears to be a good indication of such porous-layered BN nanostructures.

Acknowledgment. This work was supported by the Ministry of Science and Technology of China (Grant Nos. 2006CB605105 and 2006CB0L0601), and the National Natural Science Foundation of China.

Supporting Information Available: MD simulation results. This material is available free of charge via the Internet at http://pubs.acs.org.

JA7107678